CAPACITIVE FREQUENCY TUNING OF ALN MICROMECHANICAL RES

SAND2011-2186C

B. Kim, R.H. Olsson III, K.E. Wojciechowski
Sandia National Laboratories, Albuquerque, NM, United States of America

ABSTRACT

Frequency tuning of aluminum nitride (AlN) micromechanical resonators has been demonstrated by reactance manipulation via termination with variable capacitors. Shunting one electrode with a variable capacitor in a 13 MHz fourth overtone length-extensional mode resonator effected resonator stiffening to yield a ~600 ppm frequency shift. Tunability could be further increased by dedicating two electrodes for tuning doubling the frequency tuning range to ~1500 ppm. A tunable bandwidth balun filter has been constructed by parallel coupling of independently tunable resonators demonstrating almost three-fold increase in the bandwidth from 12 kHz to 33 kHz. Also a voltage-controlled frequency tuning printed circuit board (PCB) was implemented.

KEYWORDS

RF MEMS, resonator, tuning, aluminum nitride

INTRODUCTION

Recent advances in radio frequency microelectromechanical systems (RF MEMS) are leading a revolutionary paradigm shift in modern wireless communication technologies. In particular, AlN based overtone micromechanical resonators have achieved commercial-grade performance metrics such as low insertion loss, high $f \cdot Q$ product, and low motional impedance. Such attributes, combined with the advantages of micromachining technologies such as smaller form factor, CAD-definable frequency, cost effectiveness, and on-chip integration with transistor circuits, all these advantages make AlN -based micromechanical resonators a promising candidate for application in future generation wireless communication systems [1].

Despite all these benefits, however, there have been few reports on effective frequency tuning methods, which prevents their use in more interesting applications such as tunable bandwidth filters or frequency-tunable oscillators. At Sandia National Laboratories, we have recently reported a method of frequency tuning in AlN resonators by means of localized heating, ovenization [2]. By joule heating, the temperature of the resonator could be controlled to tune the resonant frequency. Through strategic placement of heaters and the resonator platform, its power consumption could be reduced to as low as 2.8 mW for a 4,500 ppm frequency tuning range, which is 4 times more power efficient than a previous demonstration in silicon MEMS resonators [3]. Further optimization such as anchor design can improve this power efficiency some, however, the nature of this method must consume energy to tune the resonant frequency. In addition, this approach potentially can degrade the resonator vibration sensitivity or shock resistance due to the softer anchors. Also issues with hysteresis and long-term aging are still under investigation.

In this work, we propose a new approach to tune the resonant frequencies in overtone resonators using reactive components such as capacitors and inductors. Specifically, in an overtone resonator, one or more numbers of its electrodes are terminated with variable capacitors increasing resonator stiffness to increase the resonant frequency. This approach consumes virtually zero power for frequency tuning unlike the ovenization apporach. Also it doesn't compromise the vibration sensitivity or shock resistance. The availability of such efficient tuning methods in AlN micromechanical resonators will contribute to system-level simplification and miniaturization of modern wireless communication system architectures by providing smart signal processors that can handle today's complicated multi-band frequencies with greatly reduced numbers of components.

MODELING AND ANALYSIS

Frequency tuning can be implemented by terminating one or more of the resonator electrodes with reactive components through stiffness manipulation. Figure 1*Figure 1* shows an example case when an electrode is terminated by a capacitor. At resonance, this capacitor is charged up by the induced current and impedes the resonator motion, thus stiffening the resonator to increase resonant frequency. In contrast, inductor termination leads to resonator softening to decrease resonant frequency.

This phenomenon can be also explained using a resonator equivalent electrical circuit model as shown in Fig. 2a. A mechanical resonator can be modeled using motional parameters, R_x, L_x, and C_x, and each port can be modeled as a transformer coupling between the mechanical resonator and the electrical signal. The transformer turns ratio models the number of electrodes for each port. The shunt capacitance of each port can be modeled as the summation of all the shunt capacitances of the consisting electrodes. Depending on the numbers of electrodes used for input and output, the resonator transmission motional

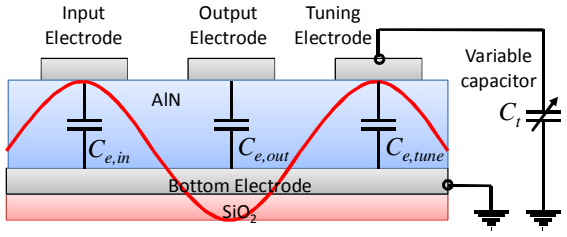

Figure 1. A concept schematic of capacitive frequency tuning in an AlN micromechanical overtone resonator. The cross-section is shown here. By terminating some electrodes with reactive components (e.g. a variable capacitor is shown here), resonant frequency can be tuned through stiffness manipulation.

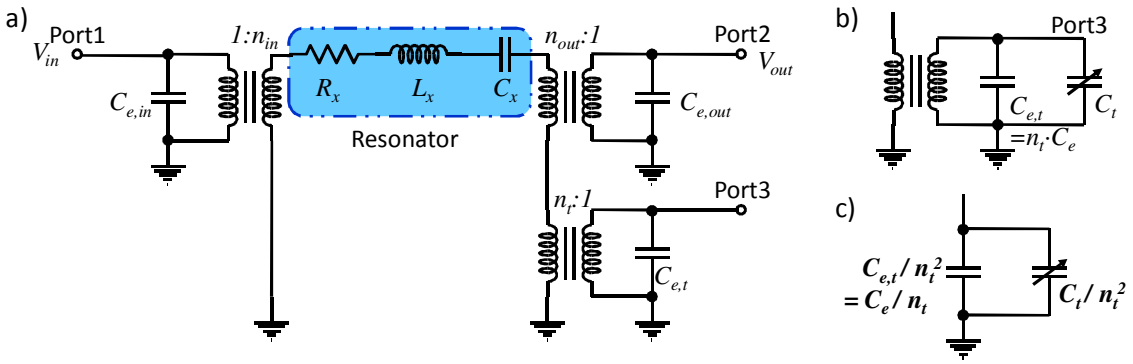

Figure 2. a) Equivalent circuit model of a resonator with multiple numbers of ports and multiple electrodes. A mechanical resonator can be modeled by motional parameters, R_x, L_x, and C_x, and each port can be modeled as a transformer coupling between the mechanical resonator and the electrical signal. The termination impedance on each electrode is reflected to the other side of the transformer by a factor of $1/n^2$. b) One port (Port 3, here) is terminated by a variable capacitor, C_t, for frequency turning. c) Equivalent circuit diagram when the impedance of the terminating capacitors is reflected to the other side of the transformer.

parameters (R_X, L_X, and C_X) can be expressed as,

$$R_X = \frac{R_x}{n_i \cdot n_o}, L_X = \frac{L_x}{n_i \cdot n_o}, C_X = n_i \cdot n_o \cdot C_x \quad (1)$$

where, n_i is the number of input electrodes and n_o is the number of output electrodes.

If a port is terminated by a variable capacitor, C_t, as shown in Fig. 2b, the impedance of this termination capacitor, together with the parallel port shunt capacitance, $C_{e,t}$, is reflected to the other side of the transformer by a factor of $1/n_t^2$ as in Fig. 2c, where, n_t is the number of electrodes for that port. Therefore, the resulting effective resonator motional capacitance, C_x', can be expressed as,

$$\frac{1}{C_x'} = \frac{1}{C_x} + \frac{n_t^2}{n_t C_e + C_t} \quad (2)$$

assuming the shunt capacitances of all the electrodes are identical to C_e.

The resulting resonator resonant frequency can be expressed as,

$$f' = \frac{1}{2\pi}\sqrt{\frac{1}{L_x C_x'}} = \frac{1}{2\pi}\sqrt{\frac{1}{L_x}\left(\frac{1}{C_x} + \frac{n_t^2}{n_t C_e + C_t}\right)} \quad (3)$$

For small changes, the change in relative resonant frequency shift can be expressed as,

$$\frac{\Delta f}{f} = \frac{1}{2}\frac{n_t^2 \cdot C_x}{n_t C_e + C_t} \quad (4)$$

Equation (4) reveals that, as C_t decreases the shift in resonant frequency increases, therefore the maximum frequency tuning occurs when C_t is 0, determined by the electrode shunt capacitance. From equation (4), the maximum tuning range can be expressed as,

$$0 < \frac{\Delta f}{f} < \frac{n_t}{2}\frac{C_x}{C_e} \quad (5)$$

assuming C_t can be varied from 0 to infinity.

Note that equation (5) predicts that the maximum tuning range is a function of the ratio between the resonator motional capacitance, C_x, and the electrode shunt capacitance, C_e, therefore the electro-mechanical coupling characteristics, k_t^2, of the aluminum nitride film sets the maximum tuning range using this method. It can be also noted that, the more electrodes that are used for signal processing, i.e., input or output, the lower the resonator transmission motional impedance, R_X, as can be seen in equation (1). In contrast, the more electrodes that are used for tuning, the wider the frequency tuning range becomes as shown in equation (4).

TEST AND MEASUREMENTS

For experimental verification of the capacitive frequency tuning method, AlN length extensional mode resonators operating in the fourth overtone were designed and fabricated as shown in the FEM mode shape and the SEM in Fig. 3. A total of four electrodes were placed on top of the resonator centered at each vibration node. The device consists of a stack of four different layers; top aluminum electrode layer, AlN transducer layer, metal electrical ground layer, and silicon dioxide layer for temperature compensation at the bottom. Resonators were fabricated in four different AlN layer thicknesses (500 nm, 750 nm, 1000 nm, and 1500 nm). The detailed fabrication process is described in [4].

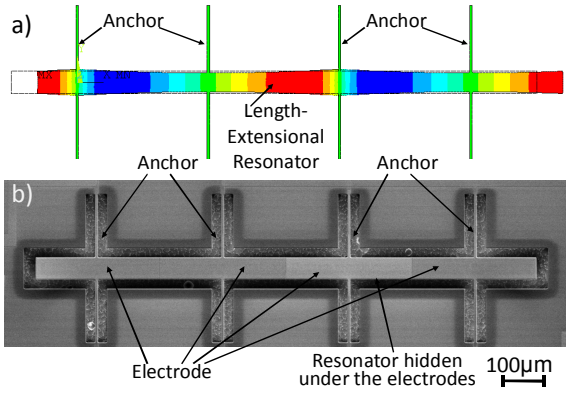

Figure 3. a) ANSYS finite element simulation of a fourth overtone length extensional resonator. Anchors are attached at the vibration nodal points. b) SEM top view of an AlN resonator. Electrodes cover the top of the resonator leaving only 2μm gaps between each other, thus the resonator structure is not visible from the top.

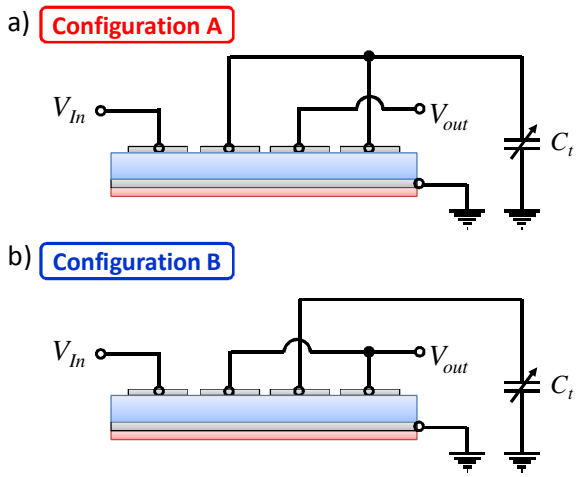

Figure 4. a)"Configuration A" utilizes one electrode for input, one for output, and two for tuning out of total four electrodes, whereas b) "Configuration B" utilizes one for input, two for output, and one for tuning.

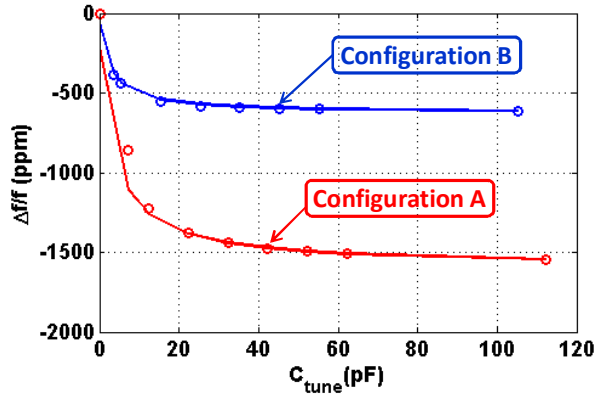

Figure 5. Tunability comparison between the two different configurations in Fig. 4. Circles are measured data points and lines are predictions from equation (4). This device was fabricated in a 1500nm-AlN film.

Frequency tunability was investigated in two configurations as illustrated in Fig. 4. Among the four electrodes, in "Configuration A," one electrode was used for input, one for output, and the remaining two for tuning. In contrast, in "Configuration B," one electrode was used for input, two for output, and only one electrode was used for tuning. While varying the value of the terminating capacitors from 0 to 100pF, the change in resonant frequency was measured. The parasitic capacitance of GSG RF probe used for attaching the capacitors was estimated as 15pF from a separate measurement.

As shown in Fig. 5, "Configuration A" exhibited almost two times wider tuning range when compared to "Configuration B," which is because twice the number of electrodes were used for tuning as predicted from equation (4). However, as shown in Fig. 6, "Configuration A" has a much larger transmission loss than "Configuration B" because the number of the electrodes used for signal processing (output electrodes here) in "Configuration A" are half of that in "Configuration B." In other words, given a total number of electrodes, to implement wider frequency tunability, more electrodes have to be used for

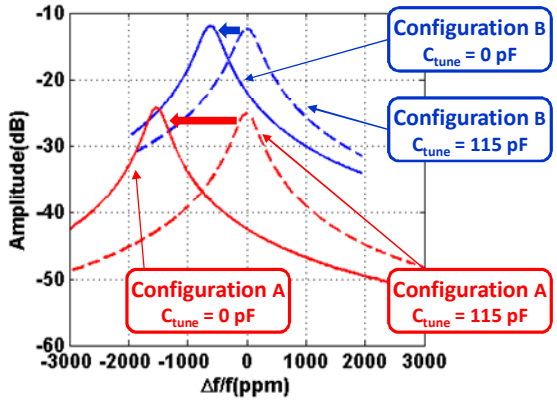

Figure 6. Frequency response of tunable resonators in two different configurations shown in Figure 4. The tested devices were fabricated in a 1500nm-thick AlN film and terminated by 50Ω-impedances..

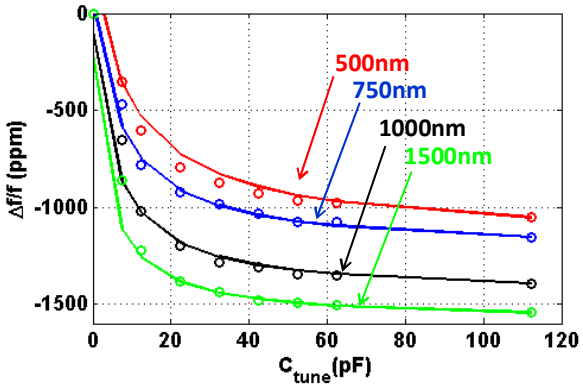

Figure 7. Tunability comparison among different film thicknesses of "Configuration A" in Figure 4. Circles are measured data points and lines are predicted from equation (4)

tuning rather than signal processing which leads to a sacrifice in the insertion loss and motional impedance.

Figure 7 shows the measured frequency shift of resonators fabricated in four different AlN film thicknesses. Resonators fabricated in thicker films have larger motional capacitance and therefore exhibit more rapid frequency change for a given tuning capacitance change as can be inferred from equation (4). The slight increases in the maximum tuning ranges with increased film thicknesses can be explained by transduction enhancement in the thicker films, as the maximum tunability is mostly dominated by the AlN electro-mechanical coupling characteristics, k_t^2, in the same electrode configurations. Table 1 summarizes resonator characteristic parameters for each thickness as well as the comparison between the measured tunabilities and predicted tunabilities using equation (4) for each film thickness.

Table 1. Comparison between predicted maximum tunability from equation (5) and measured maximum tunability as well as resonator parameters.

AlN film thickness	C_x	$C_{e,t}$	Config. A $(\Delta f/f)_{Max}$		Config. B $(\Delta f/f)_{Max}$	
			predicted	measured	predicted	measured
(nm)	(fF)	(pF)	(ppm)	(ppm)	(ppm)	(ppm)
500	7.26	5.22	518	553	1072	1052
750	4.84	3.75	566	518	1207	1154
1000	3.87	2.82	568	556	1303	1393
1500	2.71	1.96	558	612	1332	1544

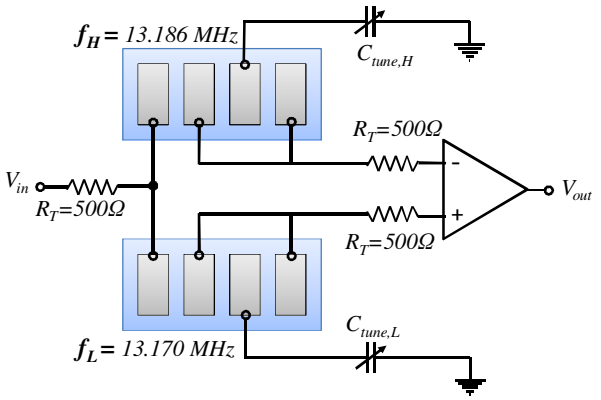

Figure 8. Schematic of a tunable bandwidth balun filter constructed by frequency tunable resonators.

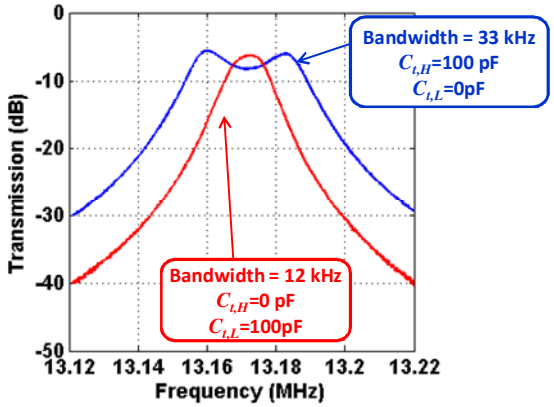

Figure 9. Frequency response of a tunable bandwidth balun filter illustrated in Figure 8. 500Ω-termination.

APPLICATIONS

In our previous work, we have demonstrated lattice balun filters through parallel coupling of multiple AlN microresonators [5]. Tunable bandwidth filters can be constructed by using frequency tunable resonators as each of the sub-resonators in the lattice balun filter. Figure 8 shows the schematic of a tunable bandwidth filter constructed by two AlN microresonators whose frequencies can be independently tuned by the capacitive tuning method. As can be seen in the frequency response plot of Fig. 9, the 3dB bandwidth of the balun filter could be tuned by almost three fold from 12 kHz to 33 kHz.

For practical applications, capacitive frequency tuning can also be implemented with voltage-controlled capacitors, varactors. Figure 10 shows the circuit diagram and printed circuit board for voltage controlled frequency tuning. The measured frequency change and quality factor with respect to the voltage change are shown in Fig. 11. The reduced frequency tuning range is due to the packaging parasitic capacitance which was measured ~3pF.

CONCLUSIONS

Frequency tuning of ~1500 ppm has been demonstrated by terminating some electrodes with a variable capacitor. By using more electrodes for tuning, the frequency tuning range can be widened, however with some sacrifice in resonator metrics such as motional impedance. The demonstrated method uses only passive electronic components such as capacitors and inductors, therefore it

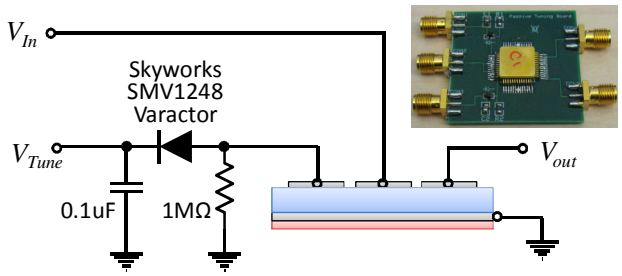

Figure 10. Schematic and PCB picture (right top corner) of voltage controlled frequency tuning circuit. A varactor was used for capacitive tuning.

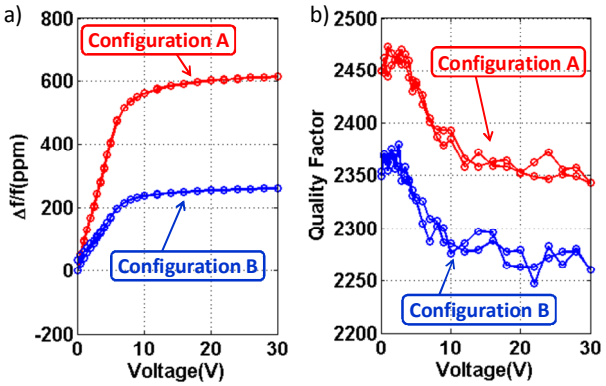

Figure 11. The measured frequency shift (a) and quality factor (b) in a voltage sweep using PCB shown in Figure 10. In the voltage sweep, no measurable hysteresis could be detected.

requires virtually zero power consumption for frequency tuning unlike previously demonstrated methods in AlN micromechanical resonators.

The maximum frequency tunability is limited by the electrode shunt capacitance, therefore by the electro-mechanical coupling, k_t^2, of the piezoelectric film. Currently research is exploring methods to improve the frequency tuning range beyond this limit.

The method demonstrated in this work can be applied to other forms of overtone resonators also. By terminating some of the electrodes placed at the vibration nodes with reactive components, resonator stiffness can be tuned resulting in frequency shift.

ACKNOWLEDGEMENT

This work was funded by DARPA ASP program. The authors would like to thank Dr. Sanjay Raman from DARPA, and R. Newgard, R. Potter, and C. Conway from Rockwell Collins for their support and guidance.

REFERENCES

[1] R. H. Olsson, et.al., in *Gov. Micro.App. and Critical Tech. Conf.*, 2010, pp. 257-260

[2] B. Kim, et.al., "Ovenized Thermally Tunable AlN Microresonators," *2010 IEEE IUS*, 2010

[3] C. M. Jha, et al., *Journal. of MEMS*, vol. 17, pp. 175-184, 2008.

[4] R. H. Olsson, et.al., in *IEEE FCS* 2007, pp. 412-419.

[5] K. E. Wojciechowski and R. H. Olson, *Hilton Head 2010*, pp. 65-69, 2010.

CONTACT

* B. Kim, tel: 1-505-844-5104; bonkim@sandia.gov